Development 134, 2569-2577 (2007) doi:10.1242/dev.003715

Ftm is a novel basal body protein of cilia involved in Shh signalling

Jeanette Vierkotten[1], Renate Dildrop[1], Thomas Peters[1,*], Baolin Wang[2] and Ulrich Rüther[1,†]

In this study we show in mice that Ftm (Rpgrip1l) is located at the ciliary basal body. Our data reveal that Ftm is necessary for developmental processes such as the establishment of left-right asymmetry and patterning of the neural tube and the limbs. The loss of Ftm affects the ratio of Gli3 activator to Gli3 repressor, suggesting an involvement of Ftm in Shh signalling. As Ftm is not essential for cilia assembly but for full Shh response, Ftm can be considered as a novel component for cilium-related Hh signalling. Furthermore, the absence of Ftm in arthropods underlines the divergence between vertebrate and *Drosophila* Hh pathways.

KEY WORDS: Basal body, Left-right asymmetry, Limb development, Mouse mutant, Neural tube

INTRODUCTION

The Hedgehog (Hh) family of secreted proteins plays an important role during embryonic development in regulating growth, patterning and morphogenesis of many tissues (Ingham and McMahon, 2001). In invertebrates, such as *Drosophila*, Hh binds its receptor Patched (Ptc) and thereby activates Smoothened (Smo), another transmembrane protein. As a consequence, processing of Cubitus interruptus (Ci) is inhibited and Ci enters the nucleus to act as a transcriptional activator. In the absence of Hh, Ci is processed and acts as a transcriptional repressor. Hh signalling in vertebrates is more complex, involving three Hh (Shh, Ihh and Dhh) and three Ci homologues (Gli1, Gli2 and Gli3). While Gli3 is known to be processed similarly to Ci, Gli2 processing in vivo is much less efficient (Dai et al., 1999; Wang et al., 2000; Pan et al., 2006). Gli3 seems to act predominantly as transcriptional repressor, while Gli2 mainly acts as activator (Ding et al., 1998; Matise et al., 1998). Gli1 appears to be an obligate activator (Dai et al., 1999). The ratio between Gli activators and repressors realizes Hh-mediated signalling (Wang et al., 2000; Briscoe and Ericson, 2001; Jacob and Briscoe, 2003).

During vertebrate development, Shh plays a crucial role in patterning of the limb buds and the neural tube. In the early limb bud, Shh regulates processing of Gli3 to lay the foundation for anteroposterior identities and the number of digits to be formed (Niswander, 2003). Shh expression in the posterior mesenchyme, within the zone of polarizing activity (ZPA), causes a Gli3 repressor gradient to form from anterior to posterior. Loss of *Shh* leads to the loss of all digits except one, reflecting the requirement of Shh function in digit formation (Chiang et al., 1996). By contrast, loss of *Gli3* leads to polydactyly and an ectopic Shh expression domain in the anterior limb bud (Masuya et al., 1995; Büscher et al., 1997). Additionally, ectopic *Shh* expression or a reduction of Gli3 repressor function has also been correlated with polydactyly (Yang et al., 1998; Wang et al., 2000).

[1]Institut für Entwicklungs- und Molekularbiologie der Tiere (EMT), Heinrich-Heine-Universität, 40225 Düsseldorf, Germany. [2]Department of Genetic Medicine, Weill Medical College of Cornell University, New York, NY 10021, USA.

*Present address: Epidauros, Biotechnologie AG, 82347 Bernried, Germany
†Author for correspondence (e-mail: ruether@uni-duesseldorf.de)

Accepted 14 May 2007

During neural tube development, Shh is initially produced by axial mesodermal cells from the notochord. The Shh signal from the notochord induces the floor plate, the ventral signalling centre of the neural tube. The floor plate in turn establishes a Shh gradient from ventral to dorsal. In response to different Shh concentrations, subsets of transcription factors are regulated, which define the five ventral neuronal subtypes: motoneurons (MN), V3, V2, V1 and V0 interneurons (Briscoe and Ericson, 2001). Based on their mode of regulation these transcription factors can be subdivided into two classes: Class I genes such as *Pax6* and *Irx3* are repressed by Shh, whereas class II genes such as *Nkx2.2* (also known as *Nkx2-2* – Mouse Genome Informatics) and *Olig2* require Shh for their expression. Additionally, the distinct progenitor domains of neuronal subtypes are refined and maintained by cross-repressive interactions between class I and class II proteins (Briscoe et al., 2000).

Cilia are specialized structures with several functions during embryonic development. They are involved in symmetry breaking within the node by producing a leftward flow and thereby causing an asymmetric distribution of signalling molecules. Analyses of different mouse mutations, such as *inversus viscerum* (*iv*) and *inversion of embryonic turning* (*inv*), revealed that both the motility of cilia and the direction of the nodal flow are necessary for the establishment of left-right asymmetry (Hirokawa et al., 2006). The role of cilia in embryonic development is eminent. Dysfunction of cilia is associated with several human disorders, such as Bardet-Biedl syndrome (BBS). This disorder is characterized by retinitis pigmentosa, renal malformations, situs inversus, cardiomyopathy, diabetes and polydactyly. Mutations in a number of genes are known to cause BBS, and there is evidence that all BBS proteins participate in a common cellular process, given that mutations in any BBS gene result in clinically related phenotypes (Katsanis, 2004; Nishimura et al., 2005; Stoetzel et al., 2006). BBS proteins are located at the basal body of cilia and centrosomes (during cell cycle), and it is proposed that these proteins assist microtubule-related transport and cellular organization processes relating to ciliary and centrosomal activities (Kim et al., 2005).

Recently, the crucial function of cilia as a specialized compartment for signal transduction has been shown. Several proteins involved in Hh-signal transduction are localized within the cilia structure. suppressor of fused (Sufu), a negative regulator of Hh signalling, and Gli proteins are localized at the distal tip of the cilia (Haycraft et al., 2005). Furthermore, Smo is enriched in cilia in the presence of Hh ligand (Corbit et al., 2005; May et al., 2005).

Genetic screens have identified additional genes required for Hh signalling and the generation of ventral neural cell types. Several of these genes are required for proper cilia formation and function [e.g. intraflagellar transport (IFT) motors kinesin-2 and Dnchc2 (Dync2h1 – Mouse Genome Informatics) and IFT particle subunits IFT88 and IFT172]. Based on phenotypic and biochemical analysis, IFT proteins seem to act downstream of the membrane-bound protein Smoothened and upstream of Gli transcription factors. They are required to generate active Gli2 in response to Hh signalling, and are required for processing of Gli3 (Scholey and Anderson, 2006). Additionally, IFT proteins are necessary for anterograde and retrograde transport, which is essential for cilia maintenance. In the absence of IFT proteins, the cilia structure fails to form (Pazour et al., 2000; Cole, 2003). Despite the finding that several proteins are essential for cilia function, the connection between cilia and Hh signalling is still only beginning to be understood.

The *Ftm* (fantom; *Rpgrip1l* – Mouse Genome Informatics) gene was originally identified in the mouse mutation *Ft* (fused toes; also known as *Fts* – Mouse Genome Informatics). This mutation is caused by a deletion of 1.6 Mb on mouse chromosome 8, affecting three members of the Iroquois family of homeobox genes, *Irx3*, *Irx5* and *Irx6*, and three other genes, named *Fts*, *Fto* (*AJ237917*) and *Ftm* (Peters et al., 2002). Development of embryos homozygous for the *Ft* mutation is delayed and embryos die between embryonic day (E) 10.5 and 14.5. The embryos show severe malformations of craniofacial and forebrain structures (van der Hoeven et al., 1994). Furthermore, they reveal polydactyly in fore limbs and syndactyly in fore- and hind limbs (Grotewold and Rüther, 2002). In addition, establishment of left-right asymmetry is disturbed, and ventral neural tube patterning and floor plate maintenance is affected (Heymer et al., 1997; Götz et al., 2005). Interestingly, the majority of these defects point to a disturbed Hh signalling, leading to the assumption that one of the genes deleted in the *Ft* mutation might be involved in Hh signalling. To clarify which of the six genes might be a component of Hh signalling, we started to generate single knockout experiments in mice. Our data reveal that the absence of Ftm seems to be the cause of the majority of defects observed in *Ft/Ft* embryos. However, some phenotypes, such as fusion of phalanges or early lethality in homozygous embryos, have not been observed, suggesting involvement of other or additional genes in these *Ft* phenotypes. The present study shows that Ftm is localized at the basal body of cilia and that it is essential for Gli protein function. We conclude that Ftm is a novel component of Hh signalling.

MATERIALS AND METHODS

Gene targeting, genotyping and PCR

We used homologous recombination to produce an *Ftm*-null allele. The targeting construct was designed to introduce a PGKneo cassette and thereby replace exon 4 and 5 of the *Ftm* coding sequence. The linearized vector was electroporated into R1 embryonic stem (ES) cells, and after G418 selection all clones were screened by Southern blot analysis. Targeted ES cells were used to create chimeras that passed the *Ftm* mutation on to their progeny. F1 animals were intercrossed to derive homozygous mutant F2 newborns and embryos by timed mating. Genotyping was carried out by either Southern blot analysis or PCR of DNA extracted from the organs or tail tips of neonates or the yolk sacs of embryos. *Gli3* mutant mice were genotyped as described (Büscher et al., 1997). Total RNA was isolated using Trizol (GibcoBRL) followed by DNaseI digestion. First strand cDNA was synthesized with the Expand RT system (Roche) according to the manufacturer's instructions. Detailed information and primer sequences are available upon request.

Western blotting

Western blot analysis was done essentially as described using anti-Gli3 antibody (Wang et al., 2000) or anti-Ftm antibody. The membrane was then incubated with anti-actin or anti-tubulin antibody (Santa Cruz) as control for loading. NIH Image was use to digitize and normalize the band intensities on scanned images.

Tissue processing and histochemistry

After dissection in ice-cold PBS, embryos were fixed in 4% paraformaldehyde for 2 to 4 hours and washed in PBS. Afterwards they were incubated in 70, 80, 90 and 100% ethanol, respectively, for 2 hours, and then 1-butanol overnight and transferred into paraffin for embedding. In situ hybridizations on paraffin sections were carried out as previously described (Moormann et al., 2001). Whole-mount RNA in situ hybridization on embryos and immunohistochemistry study on frozen tissue was performed as described (Timmer et al., 2001). Morphological stainings on sections were performed with Hematoxylin and Eosin and embryos were stained for cartilage and bones using standard Alcian Blue and Alizarin Red staining.

Cell culture

Mouse embryonic fibroblasts (MEFs) were generated from single embryos, stage E12.5 (Ftm littermates), and mesenchymal limb cells (MLCs) were generated from isolated limb buds, stage E12.5. Both were maintained in DMEM (Gibco BRL) supplemented with 10% fetal calve serum (FCS) and 1/100 (v/v) L-glutamine (Gibco BRL) and 1/100 (v/v) pen/strep (Gibco BRL) at 37°C in 5% CO_2. For Shh response analysis MLCs were incubated in DMEM (Gibco BRL) complemented with 1% fetal calve serum (FCS) and 1/100 (v/v) L-glutamine (Gibco BRL) and 1/100 (v/v) pen/strep (Gibco BRL) at 37°C in 5% CO_2 and 1 μ/ml recombinant N-Shh protein (Sigma).

Scanning electron microscopy

Scanning electron microscopy was performed as described (Sulik et al., 1994).

Antibodies

We generated polyclonal antibodies by immunizing rabbits with a GST-Ftm fusion protein encompassing the Ftm-RID domain (Pineda antibody services). Antibodies were purified with NHS sepharose (Roche) conjugated with an Ftm protein fragment containing the RID domain. Detailed information is available upon request.

We also used antibodies against acetylated α-tubulin (Sigma), γ-tubulin (Sigma), actin (Sigma), Nkx2.2, MNR2 (Hlxb9 – Mouse Genome Informatics), Shh, Pax6 (monoclonal antibodies were obtained from the Developmental Studies Hybridoma Bank developed under the auspices of the NICHD and maintained by The University of Iowa), Pax2 (Zymed) and Olig2 (Chemicon).

In silico data

Protein sequences of mouse and human *Ftm* genes and of murine Rpgrip1 were obtained from public databases (Accession number: CAC87257; NP_056087; NP_076368). Sequences of all other Ftm orthologues were derived from DNA contigs generated from raw sequence data (traces), including partial gene predictions and/or partial EST sequences.

RESULTS

Targeted mutation of Ftm

The *Ftm* gene encodes a protein of 1264 amino acids in length, which contains several protein-protein interaction domains (Fig. 1A). These comprise three coiled-coil domains, which are possibly involved in homopolymer formation (Zhao et al., 2003), one C2 domain, which is proposed to play a role in the binding of intermediate filament proteins (Gallicano et al., 1998), and a so-called RID domain. This domain was characterized in the Ftm-related protein RPGRIP1 (retinitis pigmentosa GTPase regulator interacting protein 1) (Boylan and Wright, 2000; Hong et al., 2001).

To analyse the function of *Ftm*, we generated a targeted mutation in murine ES cells by homologous recombination. The targeting construct was organized such that the mutation resulted in a

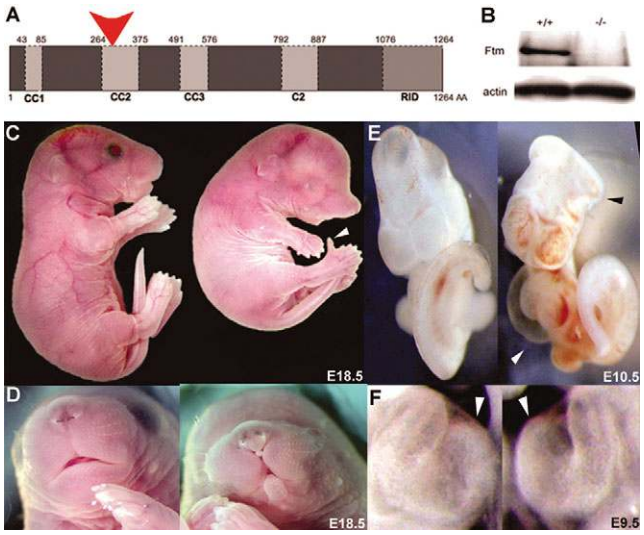

Fig. 1. The Ftm protein structure and the phenotypes of *Ftm*$^{-/-}$ embryos. (**A**) The Ftm protein contains three coiled-coil domains [CC1 amino acids (aa) 43-85, CC2 aa264-375, CC3 aa491-576], one C2 domain (aa792-887) and an RID domain (aa1076-1264). The red arrowhead marks the position where the protein is truncated due to the mutation in *Ftm* mutant mice. (**B**) Western blot analysis using an antibody raised against the C-terminus of Ftm. Ftm is absent in *Ftm*$^{-/-}$ embryos ($^{-/-}$). The lower lanes show the loading controls with anti-actin antibody. (**C-F**) *Ftm*$^{-/-}$ embryos (right side) are shown at different stages in comparison with their wild-type littermates (left side). (C) At E18.5, *Ftm* mutant embryos reveal polydactyly in fore and hind limbs (white arrowhead), reduction of eye structures and craniofacial malformations. (D) Craniofacial abnormalities in *Ftm*$^{-/-}$ embryos are shown, including a reduction of mandibular structures and unfused maxilliary and nasal tissues. (E) At E10.5, pericard enlargement (white arrowhead) and exencephaly (black arrowhead) are found in most of the embryos analysed. (F) At E9.5, 19% of analysed mutant embryos displayed dextrocardia (heart looping to the right body side) instead of the normal looping direction to the left. The final position of the ventricular part of the heart tube after looping is marked by the white arrowhead.

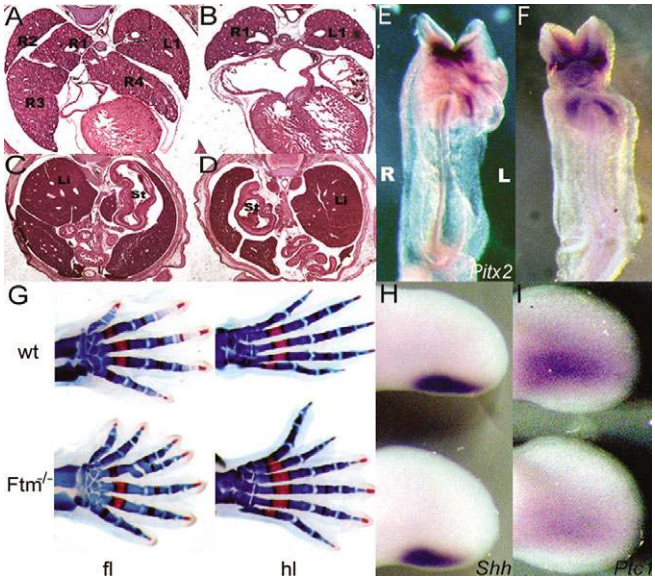

Fig. 2. Left-right asymmetry specification and limb development are affected in *Ftm*$^{-/-}$ embryos. (**A-D**) Hematoxylin and Eosin stainings at E15.5 on transverse sections. (A) In wild-type mouse embryos lungs branch into four right lobes (R1-R4) and into one left lobe (L1), while in mutant embryos (B) only two symmetric lobes are formed (R1 and L1). (C,D) In wild-type embryos the stomach develops in the left body half (C), while in some *Ftm* mutant embryos the stomach was positioned on the right (heterotaxia) (D). (**E**,**F**) Expression pattern of left-right marker gene. *Pitx2* is exclusively expressed in the left lateral plate mesoderm in wild-type embryos at the 2- to 5-somite stages (E). In *Ftm*$^{-/-}$ embryos, *Pitx2* shows a bilateral expression pattern (F). (**G**) Bone-cartilage stainings at E18.5 reveal a preaxial polydactyly in mutant limbs, visible by two extra digits in the fore limb and one extra digit in the hind limb. (**H**,**I**) At E11.5, expression of *Shh* appears to be unaffected in *Ftm* mutant limb buds (H), whereas *Ptc1* expression is reduced (I). fl, fore limb; hl, hind limb; st, stomach; wt, wild type.

truncated protein lacking all functional domains of Ftm except the first coiled-coil-domain (Fig. 1A). Ftm was not detectable in *Ftm*$^{-/-}$ embryos using antibodies raised against the C-terminus (Fig. 1B). *Ftm*$^{+/-}$ mice show no obvious phenotype. However, embryos homozygous for the *Ftm* mutation died around birth showing microphthalmia (eyes reduced in size) and a preaxial polydactyly in fore and hind limbs (Fig. 1C). Additionally, craniofacial structures were affected, including malformed mandibular structures and unfused maxilliary and nasal tissues (Fig. 1D). At earlier stages we found an enlargement of the pericard, exencephaly and disturbances in the establishment of left-right asymmetry (Fig. 1E,F). Thus, *Ftm* is required for several processes during embryonic development.

Left-right asymmetry defects in Ftm-deficient embryos

Analyses of *Ftm*$^{-/-}$ embryos between E9.5 and E11.5 revealed inversed tail turning in 39% and randomized heart looping in 19% of analysed embryos (Fig. 1F and data not shown). At later stages, histological analysis revealed heterotaxia (randomized organ position). Normally, the stomach develops in the left body half, while in several *Ftm* mutant embryos the stomach was positioned to the right (Fig. 2C,D). Additionally, 100% of *Ftm*$^{-/-}$ embryos developed only two symmetrical lung lobes (Fig. 2A,B). This left pulmonary isomerism is known from left-right mutants such as *Lefty1*$^{-/-}$ (*Ebaf*) and *Shh*$^{-/-}$, and depends on bilateral *Pitx*2 misexpression (Meno et al., 1998; Lin et al., 1999; Tsukui et al., 1999; Liu et al., 2001). To confirm the morphological observations at the molecular level, we performed whole-mount in situ hybridization and analysed the expression of left-right-specific marker genes. In wild-type embryos (2-5 somite stages), both *Pitx*2 and *Lefty*2 (*Leftb*) were expressed in the left lateral plate mesoderm (Fig. 2E; data not shown). In *Ftm*$^{-/-}$ embryos, the laterality of this expression was lost; both genes were expressed in a bilateral fashion, which indicates disturbances in early events of left-right determination (Fig. 2F; data not shown). Thus, *Ftm* is required for proper establishment of left-right asymmetry.

Loss of *Ftm* results in preaxial polydactyly and disturbances in Shh signalling

From E12.5 onwards, *Ftm*$^{-/-}$ embryos displayed a broadened shape of fore- and hind-limb buds (data not shown), suggesting a polydactylous phenotype. At later stages, this phenotype could be characterized as preaxial polydactyly (Fig. 2G). Bone cartilage stainings revealed one to two extra digits in fore limbs and one extra

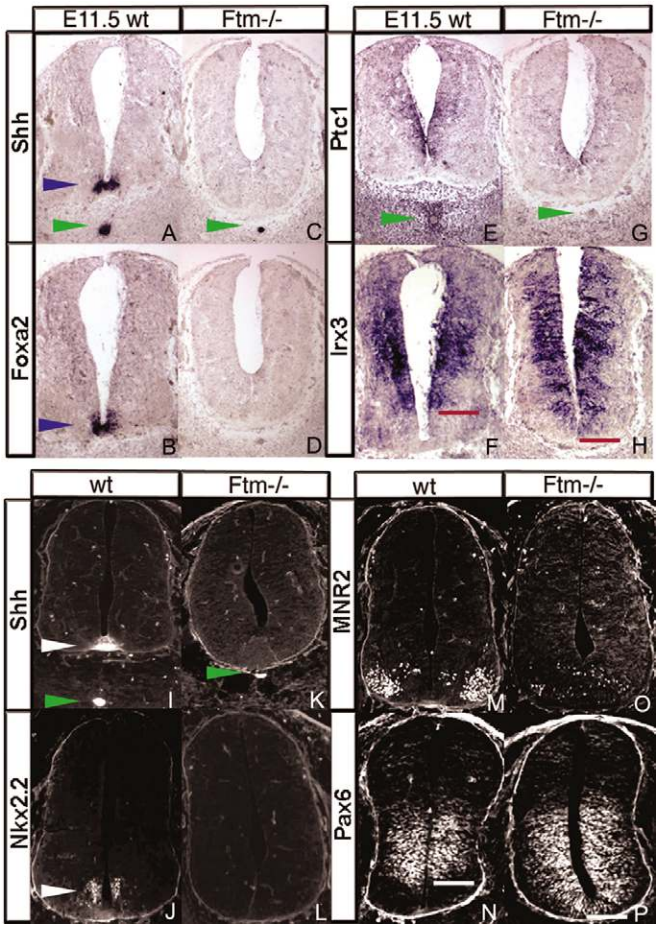

Fig. 3. Floor plate induction and ventral neural tube patterning is affected in *Ftm*$^{-/-}$ embryos. (**A-H**) In situ hybridizations on sections at stage E11.5. In the wild type mouse, *Shh* is expressed in the notochord (green arrowhead) and in the floor plate (blue arrowhead) (A), and *Foxa2* expression is restricted to the floor plate (B). In *Ftm*$^{-/-}$ embryos, *Shh* expression in the floor plate is absent (C), and *Foxa2* expression is lost (D). In wild-type embryos, *Ptc1* is expressed within the neural tube and the mesenchyme sourrounding the notochord (E), and *Irx3* is expressed within the whole neural tube except the most ventral region (F). In *Ftm*$^{-/-}$ embryos, expression of *Ptc1* is strongly reduced (G). *Irx3*-positive cells are expanded into the most ventral part of the neural tube, including the midline (expression borders are marked with red bars) (H). (**I-P**) Immunohistochemistry at stage E11.5. In wild-type embryos, Shh protein is detectable in the floor plate (white arrowhead) and notochord (green arrowhead) (I), and Nkx2.2-expressing cells are found adjacent to the floor plate (J; white arrowhead). *Ftm*$^{-/-}$ embryos show a loss of Shh protein in the floor plate (K), and Nkx2.2-expressing cells are greatly reduced (L). In the wild type, MNR2-positive cells are located in two lateral domains (M), and Pax6-expressing cells are restricted to the dorsal neural tube. In *Ftm*$^{-/-}$ embryos, only a few MNR2-postive cells are found in a spotted fashion (O), and Pax6-expressing cells are expanded into the most ventral part of the neural tube (expression borders are marked with white bars) (P).

digit in hind limbs (Fig. 2G). Known possible causes of polydactyly are ectopic expression of *Shh* and/or *Hh* activity, and *Hh* target genes *Ptc1* and *Gli1* were also previously found to be upregulated (Hui and Joyner, 1993; Yang et al., 1998). We therefore examined *Ftm* mutant limbs for ectopic expression of *Shh* and *Ptc1*. *Shh* was expressed normally in the posterior mesenchyme both, at E10.5 and E11.5 (Fig. 2H; data not shown), and no ectopic expression domain was detectable. Likewise, *Ptc1* was not ectopically expressed (Fig. 2I), suggesting a lack of increased *Hh* signalling. Moreover, *Ptc1* expression in *Ftm* mutant limb buds was reduced (Fig. 2I). The reduced number of *Ptc1* transcripts in *Ftm* mutant limb buds could be confirmed by RT-PCR analysis (see Fig. S1 in the supplementary material). These data indicate a reduction of Shh signal transduction in limb buds of *Ftm*$^{-/-}$ embryos.

Ftm is necessary for floor plate induction

To confirm that loss of Ftm leads to a reduction of Shh signalling, we analysed patterning of the neural tube, a structure allowing precise measurement of effects on Shh signalling. Shh is expressed in two ventral signalling centres along the midline, the notochord and the floor plate (Fig. 3A,I) (Roelink et al., 1995; Dodd et al., 1998). In situ hybridizations on cross sections revealed normal expression of Shh in the notochord, but a loss in the ventral neural tube (Fig. 3C). This loss was only partial along the anteroposterior axis, as demonstrated by whole-mount in situ hybridizations (see Fig. S2 in the supplementary material). Nevertheless, we were not able to detect any Shh protein in the ventral neural tube (Fig. 3K). In addition, absence of Foxa2 expression indicated a failure of successful induction of the floor plate (Fig. 3D). To test whether this failure might be the result of altered Shh signalling from the notochord, we analysed Ptc1 expression (Fig. 3G). Interestingly, we found a reduction of Ptc1 expression in the neural tube as well as in the mesenchyme surrounding the notochord, thus confirming the reduction of Shh signalling. Reduced amounts of Ptc1 expression within the neural tube were also detectable by RT-PCR (see Fig. S1 in the supplementary material).

Absence of a functional floor plate and therefore of Shh signalling was further investigated by analyses of ventral neural tube markers. Nkx2.2-positive cells are normally positioned dorsal to the floor plate and give rise to V3 interneurons (Fig. 3J). In *Ftm*$^{-/-}$ embryos, Nkx2.2-expressing cells were strongly reduced. Only in a few cases, single scattered cells were found (Fig. 3L, data not shown). MNR2 expression is indicative for motoneurons, which are normally positioned dorsolateral to the Nkx2.2 expression domains (Fig. 3M). Like Nkx2.2, MNR2 expression was strongly reduced in *Ftm* mutant embryos. MNR2-expressing cells were found in a spotted fashion also in the ventral midline (Fig. 3O). Pax6 and *Irx3* are both expressed in V0, V1 and V2 progenitors and Pax6 is additionally expressed in motoneuron progenitors (Fig. 3F,N). Both genes were found to be repressed by high amounts of *Shh* (Briscoe and Ericson, 2001). Accordingly, in *Ftm*$^{-/-}$ embryos, Pax6 and *Irx3* expression domains were expanded into the most ventral part of the neural tube (Fig. 3H,P). Thus, these results strengthen the assumption that Hh signalling is impaired in *Ftm*$^{-/-}$ embryos. Whether altered patterning of the neural tube is only a consequence of the absence of the floor plate (Shh source) or due to impairment of Hh signalling within the entire neural tube cannot be differentiated by this analysis.

Ftm acts upstream of Gli3

Gli proteins are mediators of Shh signalling and act as transcriptional repressors or activators. The outcome of Hh signalling is realized by the relative amount of Gli repressor (Gli3R) to Gli activator (Gli1, Gli2), which leads to the patterning of the neural tube (Briscoe and Ericson, 2001). Gli3R is known to antagonize floor plate induction and to block motoneuron differentiation, whereas unprocessed Gli3 does not seem to have a function in neural tube patterning (Persson et al., 2002).

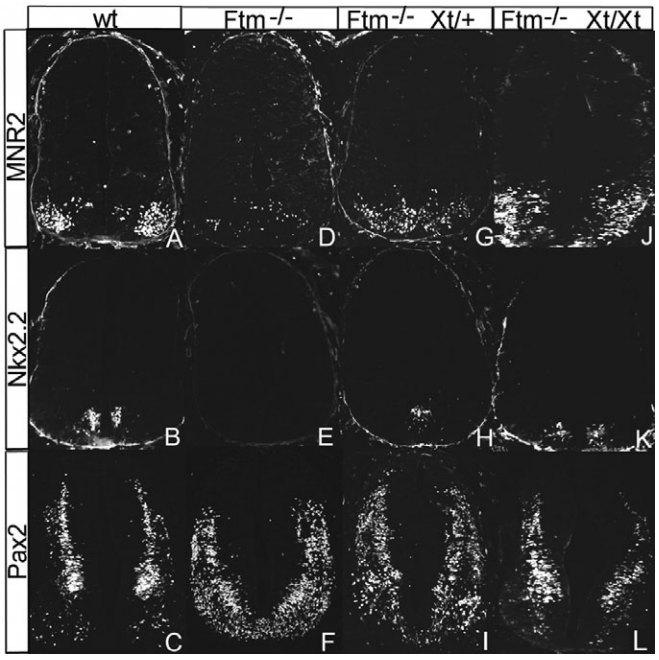

Fig. 4. Rescue of neural tube patterning in *Ftm*$^{-/-}$ embryos by abrogating Gli3 function. Shown are immunohistochemistry data at stage E11.5 mouse embryos from four different genotypes. (**A-C**) In wild-type embryos, MNR2 (A) is expressed lateral to Nkx2.2 (B), which is expressed adjacent to the floor plate. Furthermore, Pax2 is expressed in the dorsal region of the neural tube (C). (**D-F**) By contrast, *Ftm*$^{-/-}$ embryos show a strong reduction of MNR2-positive cells (D) and Nkx2.2-expressing cells (E). Expression of Pax2 is expanded into the most ventral part of the neural tube (F). (**G-I**) In *Ftm*$^{-/-}$; *Xt*/+ embryos, the number of MNR2-positive (G) and Nkx2.2-positive (H) cells is increased, but these cells still cross the midline. Pax2-expressing cells are expanded into more ventral parts within the neural tube, but there are fewer cells crossing the midline (I). (**J-L**) In *Ftm*$^{-/-}$; *Xt*/*Xt* embryos, MNR2-expressing (J) and Nkx2.2-expressing (K) cells are absent from the midline and located in two lateral distinct domains. Pax2-expressing cells (L) seem to be completely restored.

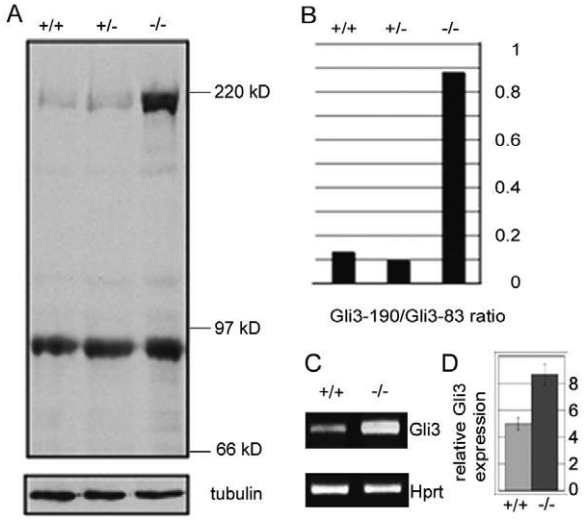

Fig. 5. Ftm is necessary for the establishment of a proper Gli3-190/Gli3-83 ratio in mice. (**A**) Immunoblots show the amounts of Gli3-190 and Gli3-83 in E11.5 embryos. In wild-type and *Ftm*$^{+/-}$ embryos, the majority of Gli3 protein was processed to form Gli3-83, and only small amounts of Gli3-190 are detectable. In *Ftm*$^{-/-}$ embryos, the amount of Gli-83 is equal to wild-type levels, but the amount of Gli3-190 is increased. Note that there is an increase in total Gli3 protein in *Ftm*$^{-/-}$ embryos. The lower part shows the loading control with anti-tubulin antibody. (**B**) Graphical evaluation of the Gli3-190/Gli3-83 ratio in wild-type, *Ftm*$^{+/-}$ and *Ftm*$^{-/-}$ embryos. At least three embryos of each genotype have been analysed. (**C**) RT-PCR analysis of RNA from E11.5 embryos. The amount of *Gli3* transcripts is increased in *Ftm*$^{-/-}$ embryos in comparison with the wild type. The lower part shows the Hprt normalization. (**D**) Comparison of relative *Gli3* transcription levels in wild-type and *Ftm*$^{-/-}$ embryos (n=3). In *Ftm*$^{-/-}$ embryos, the number of *Gli3* transcripts is increased nearly twofold.

Absence of Shh signalling has two consequences: firstly, processing of Gli3 is not inhibited (more Gli3 repressor); and secondly, Gli1 and Gli2 activation is decreased (less Gli activator). Thus, in Shh mutant embryos the loss of ventral neurons (motoneurons and several classes of interneurons) can be alleviated by abrogating Gli3 function, as shown in Shh$^{-/-}$; Gli3$^{-/-}$ combined mutant embryos (Jacob and Briscoe, 2003). If the loss of Ftm affects Shh signalling, a reduction of Gli3 in Ftm mutant embryos should rescue the observed mispatterning of the neural tube. Therefore, we crossed Ftm mutant mice with Xt mice, which carry a null allele of Gli3 (Hui and Joyner, 1993; Büscher et al., 1998). Ftm$^{-/-}$ embryos show a strong reduction of motoneurons (MNR2-positive cells) and Nkx2.2-expressing cells (Fig. 4D,E). In addition, Pax2 expression, which is negatively regulated by Shh, was found to be expanded into the most ventral part, including the midline (Fig. 4C,F). Interestingly, combined Ftm$^{-/-}$; Xt/+ embryos revealed a partial rescue of the mispatterning in the ventral neural tube. The numbers of MNR2- and Nkx2.2-positive cells increased, but were still reduced in comparison with the wild type (Fig. 4G,H). In addition, the expansion of the Pax2 domain was reduced in comparison with Ftm$^{-/-}$ embryos (Fig. 4I). Most interestingly, Ftm$^{-/-}$; Xt/Xt embryos showed a nearly complete rescue of ventral neuronal subtypes. MNR2- and Nkx2.2-expressing cells were absent from the midline and located in two distinct lateral domains (Fig. 4J,K). Furthermore, Pax2 expression seemed to be fully restored, positive cells were absent from the midline and the expression was restricted to dorsal regions (Fig. 4L). These results show that Ftm acts upstream of Gli3, and the data also confirm that Ftm is a component of Shh signalling.

To directly address the question of how Ftm may effect Gli3 function, we analysed Gli3 processing. We used an antibody against the N-terminus of Gli3 that recognizes both the Gli3 activator (Gli3-190) and repressor form (Gli3-83) (Wang et al., 2000). In both wild-type and Ftm$^{+/-}$ embryos of stage E11.5, most Gli3-190 was processed into Gli3-83, leading to high amounts of Gli3-83 and low amounts of full-length Gli3-190 (Fig. 5A). By contrast, in Ftm$^{-/-}$ embryos, the amount of Gli3-190 was dramatically increased, leading to a Gli-190:Gli-83 ratio close to 1 (Fig. 5A,B). However, the amount of Gli3-83 seems to be equal to wild-type levels. Thus, the total Gli3 protein amount seems to be increased in Ftm$^{-/-}$ embryos. We therefore analysed the levels of Gli3 RNA in mutant and wild-type embryos to see whether the increase of Gli3 protein can be correlated with increased Gli3 RNA levels. As shown by RT-PCR analysis (Fig. 5C), the Gli3-RNA level was increased in Ftm$^{-/-}$ embryos. Quantification of relative Gli3-RNA levels revealed a nearly twofold increase in the amount of Gli3 transcripts in Ftm$^{-/-}$ embryos (Fig. 5D). As Gli3 transcription is negatively regulated by Shh (Schweitzer et al.,

2000; Wang et al., 2000), the increase of the number of Gli3 transcripts confirmed the impairment of Shh signalling in Ftm$^{-/-}$ embryos.

Loss of Ftm affects cilia function

Cilia have been identified as specialized structures necessary for different developmental processes. Defects in cilia function and formation affect symmetry breaking and Shh signal transduction during embryonic development (Hirokawa et al., 2006; Scholey and Anderson, 2006). Therefore, we considered the phenotypes observed in *Ftm* mutant embryos to be caused by cilia defects. To test this hypothesis, we investigated cilia in *Ftm*$^{-/-}$ embryos. First, we examined the motile primary cilia within the node. Normally, a single cilia protrudes from the apical surface of each cell. In contrast to the wild type, the number of cilia in *Ftm* mutant embryos was found to be reduced (Fig. 6A). Cilia are also present in mesenchymal cells of the limb buds and on epithelial cells in the neural tube (Huangfu and Anderson, 2005; Haycraft et al., 2005). Staining against α-tubulin, which marks the ciliary axoneme, clearly indicated fewer cilia, both in limb buds (Fig. 6B) and in the neural tube (data not shown), suggesting disturbed cilia assembly and/or maintenance in *Ftm*$^{-/-}$ embryos.

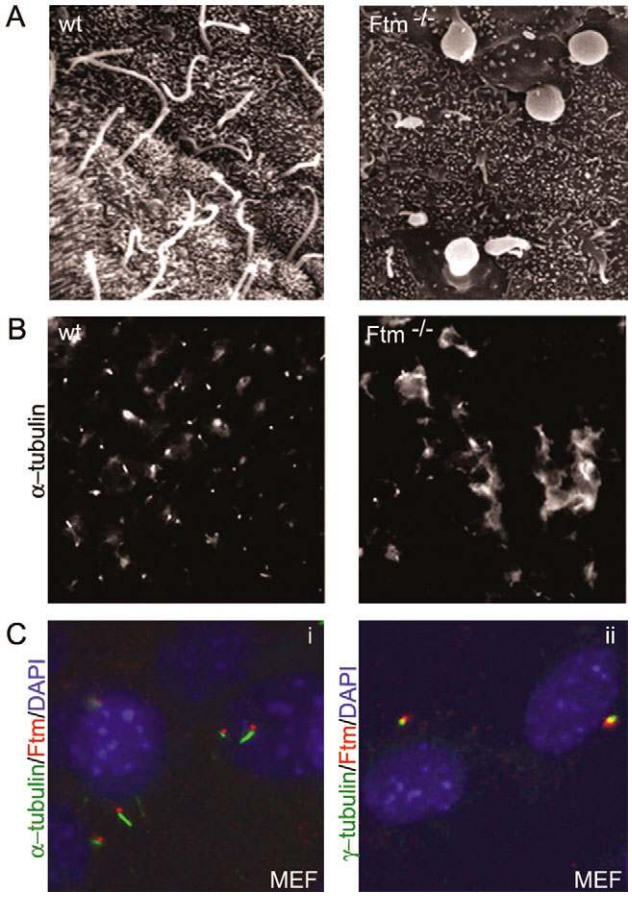

Fig. 6. Ftm is located at the basal body and is necessary for normal cilia numbers in mice. (**A**) Scanning electron microscopy images at E7.5. In the wild-type node (left), each cell possesses a single cilium on its surface, whereas in *Ftm*$^{-/-}$ embryos (right), the number of cilia is reduced and the cilia are malformed. (**B**) Immunohistochemistry on sections of limb mesenchyme at E11.5. In the wild type (left), each mesenchymal cell exhibits cilia stained by acetylated α-tubulin antibody. By contrast, in *Ftm*$^{-/-}$ embryos (right), the number of cilia is reduced. (**C**) Immunostainings on MEFs. (i) Ftm (red) is located at cilia, but does not overlap with acetylated α-tubulin (green). (ii) Ftm (red) is co-localized with γ-tubulin (green) in the basal body of the cilia. The blue staining marks the nuclei by DAPI.

Ftm is a basal body protein, highly conserved in evolution

Interestingly, use of an antibody against Ftm revealed that Ftm localizes to one end of the ciliary axoneme in MEFs (Fig. 6Ci). To clarify whether this localization is at the distal tip or at the proximal basal body of the cilia, we analysed proteins that are indicative for the basal body, such as γ-tubulin. Indeed, Ftm and γ-tubulin were found to be co-localized (Fig. 6Cii). Thus, Ftm is a component of the basal body of cilia.

As Ftm seems to be essential for cilia function in mice, we asked whether Ftm can also be found in other species. In silico analyses revealed that Ftm is conserved from cnidarians to humans (Table 1; see Fig. S3 in the supplementary material). Furthermore, Ftm shows homology to RPGRIP1, a cilium-related protein, which is found only in higher vertebrates (Table 1; see Fig. S3 in the supplementary material). Strikingly, we were not able to find Ftm in arthropods and nematodes. As it was shown for *Drosophila* that Hh signalling in this arthropod member is not associated with cilia (Huangfu and Anderson, 2006), Ftm could be one of the proteins important for the realization of this fundamental difference.

Ftm regulates Hh signalling

As shown by recent studies, loss of several cilia-associated proteins affect cilia structure and therefore Hh signalling in mammals (Huangfu and Anderson, 2005). The question arises as to whether the loss of Ftm affected Hh signalling (e.g. processing or nuclear transport) or is an indirect consequence of altering the cilia structure. To address this issue, we isolated MLCs and MEFs of wild-type and *Ftm*$^{-/-}$ embryos and measured their ability to generate cilia, which are generated in G_0 phase. The comparison of wild-type and *Ftm*$^{-/-}$ cells (both MLCs and MEFs) in G_0 phase revealed no differences in ciliogenesis: each cell developed one cilia in both wild-type and *Ftm*$^{-/-}$ cells (Fig. 7A, upper left part; data not shown). Notably, we found a slight enhancement of cilia length in *Ftm*$^{-/-}$ MLCs and MEFs (data not shown). To test whether Hh signalling was affected in *Ftm*$^{-/-}$ cells, we measured Shh responsiveness in G_0 phase of wild-type and *Ftm*$^{-/-}$ MLCs. Ciliated MLCs were incubated with Shh protein and analysed for the activation of the Hh target genes *Ptc1* and *Gli1*. In contrast to wild type, the Shh response in *Ftm*$^{-/-}$ MLCs was strongly reduced, indicated by decreased *Ptc1* and *Gli1* expression (Fig. 7A, lower left part; Fig. 7B, left panels). To test whether the Shh response is exclusively dependent on cilia, we analysed Shh target gene induction in proliferating (non-ciliated) wild-

Table 1. Homology of Ftm proteins

Mus musculus versus	% identity
Homo sapiens	89
Danio rerio	54
Branchiostoma floridae	52
Strongylocentrotus purpuratus	48
Capitalla sp.	47
Lottia gigantea	46
Nematostella vectensis	47
Hydra magnipapillata	43
Mouse Rpgrip1*	35

For the pairwise sequence comparisons, the central part of the mouse Ftm protein from aa 250 to aa 930 was used. For the multiple sequence alignment, see Fig. S3 in the supplementary material.
*Ftm-related protein.

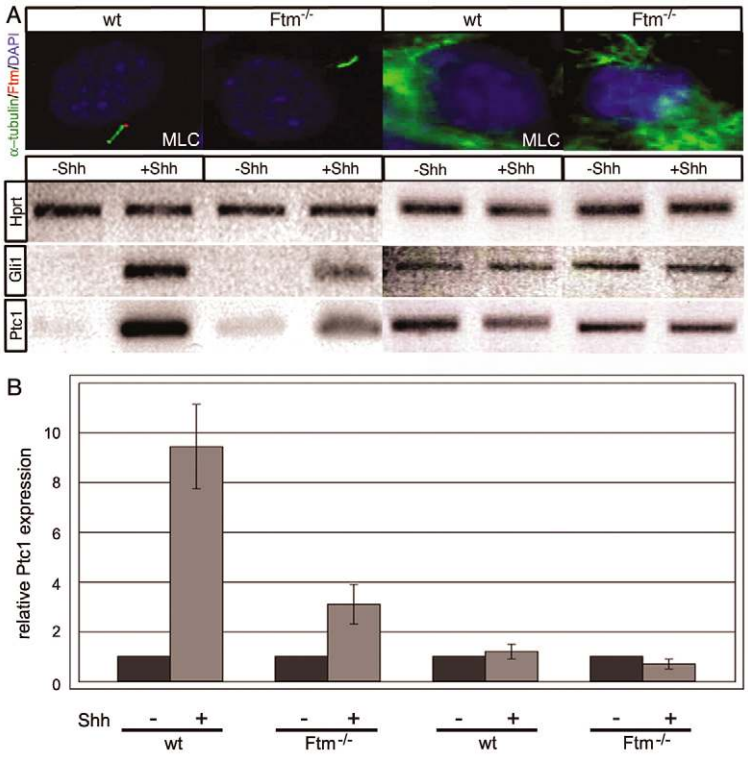

Fig. 7. Ciliogenesis and Shh signalling in *Ftm*$^{-/-}$ cells in mice. (**A**) Upper part: immunohistochemistry on G_0 phase (left) and proliferating (right) MLCs. (Left panels) In G_0 phase, each wild-type and *Ftm*$^{-/-}$ cell exhibits a single cilium, detected by acetylated α-tubulin antibody (green staining). Ftm (stained in red) is present only in wild-type MLCs. (Right panels) In proliferating wild-type and *Ftm*$^{-/-}$ MLCs, cilia are absent and the cytoplasm is enriched with cytoskeletal tubulins, marked by acetylated α-tubulin antibody (green staining). Note that Ftm antibodies were not used in this staining. Lower part: Shh response in G_0-phase (left) and proliferating (right) wild-type and *Ftm*$^{-/-}$ MLCs. G_0-phase wild-type MLCs show a strong induction of *Gli1* and *Ptc1* after incubation with recombinant Shh protein for 24 hours. In G_0-phase *Ftm*$^{-/-}$ MLCs, the induction of *Gli1* and *Ptc1* is strongly reduced. Both, proliferating (non-ciliated) wild-type and *Ftm*$^{-/-}$ MLCs show no induction of Shh target genes after stimulation. (**B**) Quantification of *Ptc1*-expression levels in G_0-phase (left panels) and proliferating (right panels) wild-type and *Ftm*$^{-/-}$ MLCs after Shh stimulation. The quantification of *Ptc1* induction reveals that G_0-phase wild-type MLCs show an increase of *Ptc1* transcripts by a factor of 9.4, whereas G_0-phase *Ftm*$^{-/-}$ MLCs show an increase of only a factor of 3.1. Proliferating (non-ciliated) wild-type and *Ftm*$^{-/-}$ MLCs show no changes in the relative expression levels of *Ptc1* upon treatment with Shh (wild-type MLCs 1.1; *Ftm*$^{-/-}$ MLCs 0.8). Data represent the quantification of three independent experiments. wt, wild type.

type and *Ftm*$^{-/-}$ MLCs (Fig. 7A,B right). Both wild-type and *Ftm*$^{-/-}$ MLCs showed no induction of Shh target genes after stimulation with Shh (Fig. 7A, right panels; Fig. 7B, right panels). These data confirm that Shh signals are exclusively transduced by cilia and that the remaining induction of Shh targets in *Ftm*$^{-/-}$ MLCs is cilia-dependent. Furthermore, loss of Ftm does not affect ciliogenesis and does not completely abolish Shh signalling. However, loss of Ftm severely interferes with the efficiency of signal transduction. Thus, Ftm is necessary for normal cilium-related Shh signalling.

DISCUSSION

In this study we show that Ftm is a protein located at the basal body of cilia. Nevertheless, in the absence of Ftm, primary cells were still able to generate cilia on every cell. However, the induction of Shh target genes was reduced to 30% in these *Ftm*$^{-/-}$ cells. As induction of *Ptc1* and *Gli1* was absolutely dependent on the presence of cilia, we conclude that Ftm is an integral part of the cilia-associated signal transduction cascade necessary to elicit a quantitative Shh response. This relation of Ftm to Shh signalling is in line with the phenotypic changes detectable in *Ftm*$^{-/-}$ embryos.

Impaired Hh signalling in Ftm$^{-/-}$ embryos

All observed midline defects in *Ftm*$^{-/-}$ embryos (e.g. randomized heart looping, left-lung isomerism, dorsalization of the neural tube) can be explained by a reduction or absence of Hh signalling, similar to the phenotypes described for *Shh*$^{-/-}$ embryos (Chiang et al., 1996; Tsukui et al., 1999). To provide detailed evidence for this interpretation, we investigated patterning of the neural tube, a structure extensively used for quantitative and qualitative studies of Shh function (Briscoe and Ericson, 2001; Jacob and Briscoe, 2003). Although *Shh* was expressed in the notochord throughout development we were not able to detect Shh in the neural tube from E10.5 onwards, a phenomenon also described for IFT mutant mice that lack cilia and therefore functional Shh signalling (Huangfu et al., 2003; Haycraft et al., 2005; Liu et al., 2005). As a consequence, the neural tube of *Ftm*$^{-/-}$ embryos was mispatterned in a similar way to that seen in IFT mutant embryos: the floor plate was lost, and consequently motoneurons and V3 neurons were reduced. Furthermore, it had been shown previously that mispatterning of the neural tube in polaris (*Ift88*) and wimple (*Ift172*) mutant mice could partially be rescued by depletion of Gli3 in combined mutant embryos (Huangfu et al., 2003). The same partial rescue was also found in *Ftm*$^{-/-}$; *Gli3*$^{-/-}$ combined mutant embryos, suggesting a similar mechanism. Biochemical analyses revealed that mutations in IFT genes (e.g. polaris) negatively influence Gli3 processing. In addition, Gli activator function and Shh response was impaired (Haycraft et al., 2005; Liu et al., 2005; May et al., 2005). Analysis of MLCs of polaris mutant mice showed a complete loss of Shh responsiveness and a failure of Hh target gene activation by Gli2 (Haycraft et al., 2005). Similarly, we could show that Shh responsiveness is strongly reduced in *Ftm*$^{-/-}$ embryos and in cultured MLCs. Therefore, in *Ftm*$^{-/-}$ embryos, reduced activator function due to a reduction in Shh responsiveness, in combination with remaining Gli3 repressor function, leads to the same mispatterning of the neural tube as that in IFT mutant mice.

In contrast to neural tube patterning, limb development is rather indifferent to Gli activator function. Mutations in Gli1 and Gli2 have no effect on limb patterning, whereas loss of Gli3 dramatically changes digit number and identity. The major mediator in limb patterning is Gli3-83 (Niswander, 2003). A complete loss of Gli3-83 causes a severe polydactyly (two to three extra digits) and leads to a complete loss of digit identity (Niswander, 2003). The defects in *Ftm*$^{-/-}$ and IFT mutant embryos were much less severe. In *Ftm*$^{-/-}$ limbs only one to two extra digits were formed, with a clear digit identity, and in IFT mutant embryos a polydactyly comparable to *Ftm*$^{-/-}$ embryos was described (Haycraft et al., 2005; Liu et al., 2005). The polydactylous phenotype of IFT mutant mice appears to be a consequence of the change in the ratio of Gli3-190 to Gli3-83,

due to impaired Gli3 processing. Although our western blot analysis revealed equal levels of Gli3-83 in *Ftm*$^{-/-}$ and wild-type embryos, the ratio of Gli3-190 to Gli3-83 is changed due to an increased amount of Gli3-190. A recent study by Wang et al. (Wang et al., 2007) supports this interpretation.

Ftm and cilium-related Hh signalling

Ftm and IFT proteins are both necessary for proper Hh signalling, but strikingly they show quantitative differences in Shh responsiveness. A loss of Ftm leads to a strong reduction of Shh responsiveness in MLCs, whereas a loss of polaris causes a complete loss of Shh responsiveness (Haycraft et al., 2005). Furthermore, in contrast to polaris mutant embryos (Haycraft et al., 2005), *Ftm*$^{-/-}$ cells possess cilia, which are detectable by antibodies against acetylated α-tubulin. In addition, and again in contrast to polaris mutant cells, 100% of *Ftm*$^{-/-}$ MLCs in culture do generate cilia. Thus, Ftm is not necessary for the generation of cilia but rather for allowing efficient cilia-dependent Shh response. As we noticed slight changes in the architecture of *Ftm*$^{-/-}$ cilia, Ftm might also play a role in the stability or shape of cilia, which could have consequences on the half-life of the cilia. However, our cell culture experiments did not give any indication for this hypothesis.

IFT function is necessary for proper Gli3 processing and thereby increases the amount of Gli3-190 and decreases the amount of Gli3-83. A loss of Ftm seems not to affect the efficiency of processing. In *Ftm*$^{-/-}$ embryos the Gli3-83 level appears to be normal and the amount of Gli3-190 is increased due to increased *Gli3* expression. Nevertheless, the consequences are the same: changes in the ratio of Gli3-190 to Gli3-83 in IFT mutants and *Ftm*$^{-/-}$ embryos result in a reduced expression of Hh target genes (such as *Ptc1*), a polydactylous phenotype and dorsalization of the neural tube (May et al., 2005; Haycraft et al., 2005). In both cases Hh signalling is impaired and would be expected to lead to an increase of *Gli3* expression (Schweitzer et al., 2000; Wang et al., 2000). So far this has been shown only for *Ftm*-negative embryos.

Ftm and its relative RPGRIP1

Sequence analysis revealed Ftm to be homologous to RPGRIP1. Mutations of RPGRIP1 cause the human disorder retinitis pigmentosa, a degeneration of photoreceptor cells (Mavlyutov et al., 2002; Pawlyk et al., 2005). RPGRIP1 functions in photoreceptor cells in the retina, especially at the connecting cilium between the outer and inner segment. RPGRIP1 anchors RPGR (retinitis pigmentosa GTPase regulator) to the basal body of this connecting cilium. This interaction is necessary for cilia stability and retroflagellar transport (Boylan and Wright, 2000; Hong et al., 2001; Zhao et al., 2003). Absence of RPGRIP1 in mice and humans results in retinitis pigmentosa, suggesting a function of this protein in maintaining the integrity of this specialized cilium-related structure (Pawlyk et al., 2005). The loss of Ftm causes malformations of cilia in specific tissues such as the node, and also leads to a reduction in cilia number. Therefore, Ftm could be necessary for cilia maintenance in a similar fashion. However isolated primary cells (MLCs and MEFs) showed no reduction in cilia number and only moderate malformations of the cilia structure, which clearly shows that Ftm is not essential for ciliogenesis. Interestingly, certain tissues, such as trachea and olfactory epithelium, in *Ftm*$^{-/-}$ embryos show no changes in cilia number (Ulrich Dirks and U.R., unpublished). Thus, cilia are reduced only in structures/tissues in which morphogenetic processes take place. This finding suggests that a fully functional cilia-coupled signalling pathway is necessary for cilia maintenance.

Our phylogenetic analysis revealed that Ftm exists in nearly all species from cnidarians to vertebrates. The homology constitutes from 42% in hydra to 89% in humans, implying that Ftm is highly conserved in evolution. By contrast, RPGRIP1 is present only in vertebrates, and detailed analysis identified Ftm as phylogenetic ancestor of RPGRIP1 (data not shown). RPGRIP1 is exclusively expressed in the eye, whereas Ftm is ubiquitously expressed, stressing the importance of Ftm in general cilium function. Surprisingly, we were not able to detect Ftm homologues in arthropods and nematodes. In arthropods such as *Drosophila*, cilia are present only in specific neuronal subtypes and in sperm cells (Basto et al., 2006). The connection between Hh signalling and cilia in arthropods has yet not been shown, suggesting that Ftm plays a specific role in Hh signal transduction in association with cilia. As loss of Ftm leads to a quantitative impairment of the Hh response, we speculate that a subset of basal body proteins is essential for cilia to gain the ability to elicit a full and robust Shh responsiveness. Ftm seems to be one of these proteins, and thus may be used as an entry point to investigate vertebrate-specific Hh signalling.

We thank Jürgen Knobloch, Julia Fischer and Patrick Hill for critical reading of the manuscript. Furthermore, we thank Rüdiger Riehl for electron microscope imaging. This work was supported by the DFG (SFB 590) to U.R. and an NIH grant to B.W. (R01 CA111673).

Supplementary material

Supplementary material for this article is available at http://dev.biologists.org/cgi/content/full/134/14/2569/DC1

References

Basto, R., Lau, J., Vinogradova, T., Gardiol, A., Woods, C. G., Khodjakov, A. and Raff, J. W. (2006). Flies without centrioles. *Cell* **125**, 1375-1386.
Boylan, J. P. and Wright, A. F. (2000). Identification of a novel protein interacting with RPGR. *Hum. Mol. Genet.* **9**, 2085-2093.
Briscoe, J. and Ericson, J. (2001). Specification of neuronal fates in the ventral neural tube. *Curr. Opin. Neurobiol.* **11**, 43-49.
Briscoe, J., Pierani, A., Jessell, T. M. and Ericson, J. (2000). A homeodomain protein code specifies progenitor cell identity and neuronal fate in the ventral neural tube. *Cell* **101**, 435-445.
Büscher, D., Bosse, B., Heymer, J. and Rüther, U. (1997). Evidence for genetic control of Sonic hedgehog by Gli3 in mouse limb development. *Mech. Dev.* **62**, 175-182.
Büscher, D., Grotewold, L. and Rüther, U. (1998). The XtJ allele generates a Gli3 fusion transcript. *Mamm. Genome* **9**, 676-678.
Chiang, C., Litingtung, Y., Lee, E., Young, K. E., Corden, J. L., Westphal, H. and Beachy, P. A. (1996). Cyclopia and defective axial patterning in mice lacking Sonic hedgehog gene function. *Nature* **383**, 407-413.
Cole, D. G. (2003). The intraflagellar transport machinery of Chlamydomonas reinhardtii. *Traffic* **4**, 435-442.
Corbit, K. C., Aanstad, P., Singla, V., Norman, A. R., Stainier, D. Y. and Reiter, J. F. (2005). Vertebrate Smoothened functions at the primary cilium. *Nature* **437**, 1018-1021.
Dai, P., Akimaru, H., Tanaka, Y., Maekawa, T., Nakafuku, M. and Ishii, S. (1999). Sonic Hedgehog-induced activation of the Gli1 promoter is mediated by GLI3. *J. Biol. Chem.* **274**, 8143-8152.
Ding, Q., Motoyama, J., Gasca, S., Mo, R., Sasaki, H., Rossant, J. and Hui, C. C. (1998). Diminished Sonic hedgehog signalling and lack of floor plate differentiation in Gli2 mutant mice. *Development* **125**, 2533-2543.
Dodd, J., Jessell, T. M. and Placzek, M. (1998). The when and where of floor plate induction. *Science* **282**, 1654-1657.
Gallicano, G. I., Kouklis, P., Bauer, C., Yin, M., Vasioukhin, V., Degenstein, L. and Fuchs, E. (1998). Desmoplakin is required early in development for assembly of desmosomes and cytoskeletal linkage. *J. Cell Biol.* **143**, 2009-2022.
Götz, K., Briscoe, J. and Rüther, U. (2005). Homozygous Ft embryos are affected in floor plate maintenance and ventral neural tube patterning. *Dev. Dyn.* **233**, 623-630.
Grotewold, L. and Rüther, U. (2002). The Fused toes (Ft) mouse mutation causes anteroposterior and dorsoventral polydactyly. *Dev. Biol.* **251**, 129-141.
Haycraft, C. J., Banizs, B., Aydin-Son, Y., Zhang, Q., Michaud, E. J. and Yoder, B. K. (2005). Gli2 and Gli3 localize to cilia and require the intraflagellar transport protein polaris for processing and function. *PLoS Genet.* **1**, e53.
Heymer, J., Kuehn, M. and Rüther, U. (1997). The expression pattern of nodal and lefty in the mouse mutant Ft suggests a function in the establishment of handedness. *Mech. Dev.* **662**, 5-11.

Hirokawa, N., Tanaka, Y., Okada, Y. and Takeda, S. (2006). Nodal flow and the generation of left-right asymmetry. *Cell*. **125**, 33-45.
Hong, D. H., Yue, G., Adamian, M. and Li, T. (2001). Retinitis pigmentosa GTPase regulator (RPGRr)-interacting protein is stably associated with the photoreceptor ciliary axoneme and anchors RPGR to the connecting cilium. *J. Biol. Chem*. **276**, 12091-12099.
Huangfu, D. and Anderson, K. V. (2005). Cilia and Hedgehog responsiveness in the mouse. *Proc. Natl. Acad. Sci. USA* **102**, 11325-11330.
Huangfu, D. and Anderson, K. V. (2006). Signalling from Smo to Ci/Gli: conservation and divergence of Hedgehog pathways from Drosophila to vertebrates. *Development* **133**, 3-14.
Huangfu, D., Liu, A., Rakeman, A. S., Murcia, N. S., Niswander, L. and Anderson, K. V. (2003). Hedgehog signalling in the mouse requires intraflagellar transport proteins. *Nature* **426**, 83-87.
Hui, C. C. and Joyner, A. L. (1993). A mouse model of greig cephalopolysyndactyly syndrome: the extra-toesJ mutation contains an intragenic deletion of the Gli3 gene. *Nat. Genet*. **3**, 241-246.
Ingham, P. W. and McMahon, A. P. (2001). Hedgehog signalling in animal development: paradigms and principles. *Genes Dev*. **15**, 3059-3087.
Jacob, J. and Briscoe, J. (2003). Gli proteins and the control of spinal-cord patterning. *EMBO Rep*. **4**, 761-765.
Katsanis, N. (2004). The oligogenic properties of Bardet-Biedl syndrome. *Hum. Mol. Genet*. **13**, R65-R71.
Kim, J. C., Ou, Y. Y., Badano, J. L., Esmail, M. A., Leitch, C. C., Fiedrich, E., Beales, P. L., Archibald, J. M., Katsanis, N., Rattner, J. B. et al. (2005). MKKS/BBS6, a divergent chaperonin-like protein linked to the obesity disorder Bardet-Biedl syndrome, is a novel centrosomal component required for cytokinesis. *J. Cell Sci*. **118**, 1007-1020.
Lin, C. R., Kioussi, C., O'Connell, S., Briata, P., Szeto, D., Liu, F., Izpisua-Belmonte, J. C. and Rosenfeld, M. G. (1999). Pitx2 regulates lung asymmetry, cardiac positioning and pituitary and tooth morphogenesis. *Nature* **401**, 279-282.
Liu, A., Wang, B. and Niswander, L. A. (2005). Mouse intraflagellar transport proteins regulate both the activator and repressor functions of Gli transcription factors. *Development* **132**, 3103-3111.
Liu, C., Liu, W., Lu, M. F., Brown, N. A. and Martin, J. F. (2001). Regulation of left-right asymmetry by thresholds of Pitx2c activity. *Development* **128**, 2039-2048.
Masuya, H., Sagai, T., Wakana, S., Moriwaki, K. and Shiroishi, T. (1995). A duplicated zone of polarizing activity in polydactylous mouse mutants. *Genes. Dev*. **9**, 1645-1653.
Matise, M. P., Epstein, D. J., Park, H. L., Platt, K. A. and Joyner, A. L. (1998). Gli2 is required for induction of floor plate and adjacent cells, but not most ventral neurons in the mouse central nervous system. *Development* **125**, 2759-2770.
Mavlyutov, T. A., Zhao, H. and Ferreira, P. A. (2002). Species-specific subcellular localization of RPGR and RPGRIP isoforms: implications for the phenotypic variability of congenital retinopathies among species. *Hum. Mol. Genet*. **11**, 1899-1907.
May, S. R., Ashique, A. M., Karlen, M., Wang, B., Shen, Y., Zarbalis, K., Reiter, J., Ericson, J. and Peterson, A. S. (2005). Loss of the retrograde motor for IFT disrupts localization of Smo to cilia and prevents the expression of both activator and repressor functions of Gli. *Dev. Biol*. **287**, 378-389.
Meno, C., Shimono, A., Saijoh, Y., Yashiro, K., Mochida, K., Ohishi, S., Noji, S., Kondoh, H. and Hamada, H. (1998). lefty-1 is required for left-right determination as a regulator of lefty-2 and nodal. *Cell* **94**, 287-297.
Moorman, A. F., Houweling, A. C., de Boer, P. A. and Christoffels, V. M. (2001). Sensitive nonradioactive detection of mRNA in tissue sections: novel application of the whole-mount in situ hybridization protocol. *J. Histochem. Cytochem*. **49**, 1-8.
Nishimura, D. Y., Swiderski, R. E., Searby, C. C., Berg, E. M., Ferguson, A. L., Hennekam, R., Merin, S., Weleber, R. G., Biesecker, L. G., Stone, E. M. et al. (2005). Comparative genomics and gene expression analysis identifies BBS9, a new Bardet-Biedl syndrome gene. *Am. J. Hum. Genet*. **77**, 1021-1033.
Niswander, L. (2003). Pattern formation: old models out on a limb. *Nat. Rev. Genet*. **4**, 133-143.
Pan, Y., Bai, C. B., Joyner, A. L. and Wang, B. (2006). Sonic hedgehog signalling regulates Gli2 transcriptional activity by suppressing its processing and degradation. *Mol. Cell. Biol*. **26**, 3365-3377.
Pawlyk, B. S., Smith, A. J., Buch, P. K., Adamian, M., Hong, D. H., Sandberg, M. A., Ali, R. R. and Li, T. (2005). Gene replacement therapy rescues photoreceptor degeneration in a murine model of Leber congenital amaurosis lacking RPGRIP. *Invest. Ophthalmol. Vis. Sci*. **46**, 3039-3045.
Pazour, G. J., Dickert, B. L., Vucica, Y., Seeley, E. S., Rosenbaum, J. L., Witman, G. B. and Cole, D. G. (2000). Chlamydomonas IFT88 and its mouse homologue, polycystic kidney disease gene tg737, are required for assembly of cilia and flagella. *J. Cell Biol*. **151**, 709-718.
Persson, M., Stamataki, D., te Welscher, P., Andersson, E., Böse, J., Rüther, U., Ericson, J. and Briscoe, J. (2002). Dorsal-ventral patterning of the spinal cord requires Gli3 transcriptional repressor activity. *Genes Dev*. **16**, 2865-2878.
Peters, T., Ausmeier, K., Dildrop, R. and Rüther, U. (2002). The mouse Fused toes (Ft) mutation is the result of a 1.6-Mb deletion including the entire Iroquois B gene cluster. *Mamm. Genome* **13**, 186-188.
Roelink, H., Porter, J. A., Chiang, C., Tanabe, Y., Chang, D. T., Beachy, P. A. and Jessell, T. M. (1995). Floor plate and motor neuron induction by different concentrations of the amino-terminal cleavage product of sonic hedgehog autoproteolysis. *Cell* **81**, 445-455.
Scholey, J. M. and Anderson, K. V. (2006). Intraflagellar transport and cilium-based signalling. *Cell* **125**, 439-442.
Schweitzer, R., Vogan, K. J. and Tabin, C. J. (2000). Similar expression and regulation of Gli2 and Gli3 in the chick limb bud. *Mech. Dev*. **98**, 171-174.
Stoetzel, C., Laurier, V., Davis, E. E., Muller, J., Rix, S., Badano, J. L., Leitch, C. C., Salem, N., Chouery, E., Corbani, S. et al. (2006). BBS10 encodes a vertebrate-specific chaperonin-like protein and is a major BBS locus. *Nat. Genet*. **38**, 727.
Sulik, K., Dehart, D. B., Iangaki, T., Carson, J. L., Vrablic, T., Gesteland, K. and Schoenwolf, G. C. (1994). Morphogenesis of the murine node and notochordal plate. *Dev. Dyn*. **201**, 260-278.
Timmer, J., Johnson, J. and Niswander, L. (2001). The use of in ovo electroporation for the rapid analysis of neural-specific murine enhancers. *Genesis* **29**, 123-132.
Tsukui, T., Capdevila, J., Tamura, K., Ruiz-Lozano, P., Rodriguez-Esteban, C., Yonei-Tamura, S., Magallon, J., Chandraratna, R. A., Chien, K., Blumberg, B. et al. (1999). Multiple left-right asymmetry defects in Shh$^{(-/-)}$ mutant mice unveil a convergence of the shh and retinoic acid pathways in the control of Lefty-1. *Proc. Natl. Acad. Sci. USA* **96**, 11376-11381.
van der Hoeven, F., Schimmang, T., Volkmann, A., Mattei, M. G., Kyewski, B. and Rüther, U. (1994). Programmed cell death is affected in the novel mouse mutant Fused toes (Ft). *Development* **120**, 2601-2607.
Wang, B., Fallon, J. F. and Beachy, P. A. (2000). Hedgehog-regulated processing of Gli3 produces an anterior/posterior repressor gradient in the developing vertebrate limb. *Cell* **100**, 423-434.
Wang, C., Rüther, U. and Wang, B. (2007). The Shh-independent activator function of full-length Gli3 protein and its role in vertebrate limb digit patterning. *Dev. Biol*. **305**, 460-469.
Yang, Y., Guillot, P., Boyd, Y., Lyon, M. F. and McMahon, A. P. (1998). Evidence that preaxial polydactyly in the Doublefoot mutant is due to ectopic Indian Hedgehog signalling. *Development* **125**, 3123-3132.
Zhao, Y., Hong, D. H., Pawlyk, B., Yue, G., Adamian, M., Grynberg, M., Godzik, A. and Li, T. (2003). The retinitis pigmentosa GTPase regulator (RPGR)-interacting protein: subserving RPGR function and participating in disk morphogenesis. *Proc. Natl. Acad. Sci. USA* **100**, 3965-3970.